Evaluation of Oxidation Damage in Thermal Barrier Coating Systems

Dongming Zhu and Robert A. Miller
Lewis Research Center
Cleveland, Ohio

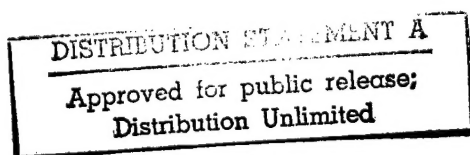19970124 107

National Aeronautics and
Space Administration

DTIC QUALITY INSPECTED 3

U.S. ARMY

RESEARCH LABORATORY

EVALUATION OF OXIDATION DAMAGE IN THERMAL BARRIER COATING SYSTEMS

Dongming Zhu † and Robert A. Miller
National Aeronautics and Space Administration
Lewis Research Center, Cleveland, OH 44135

ABSTRACT

A method based on the technique of dilatometry has been established to quantitatively evaluate the interfacial damage due to the oxidation in a thermal barrier coating system. Strain isolation and adhesion coefficients have been proposed to characterize the thermal barrier coating (TBC) performance based on its thermal expansion behavior. It has been found that, for a thermal barrier coating system consisting of ZrO_2-$8\%Y_2O_3$/FeCrAlY/4140 steel substrate, the oxidation of the bond coat and substrate significantly reduced the ceramic coating adherence, as inferred from the dilatometry measurements. The *in-situ* thermal expansion measurements under 30°C to 700°C thermal cycling in air showed that the adhesion coefficient, A_i, decreased by 25% during the first 35 oxidation cycles. Metallography showed that delamination occurred at both the ceramic/bond coat and bond coat/substrate interfaces. In addition, the strain isolation effect has been improved by increasing the FeCrAlY bond coat thickness. The strain isolation coefficient, S_i, increased from about 0.04 to 0.25, as the bond coat thickness changed from 0.1 mm to 1.0 mm. It may be possible to design optimum values of strain isolation and interface adhesion coefficients to achieve the best TBC performance.

Keywords: Thermal Barrier Coating, Dilatometry, Thermal Expansion, Interface Adhesion, Oxidation Damage, Strain Isolation

INTRODUCTION

Plasma-sprayed ceramic thermal barrier coatings (TBC) have been developed for advanced gas turbine [1-3] and diesel engine components [4-6] to improve engine reliability and fuel efficiency. A typical TBC coating system consists of a top layer ZrO_2-$8\%Y_2O_3$ coating and an intermediate MCrAlY bond coat on the alloy substrate. The failure mechanism of TBC is very complicated. In general the coating failure is closely related to thermal stresses induced from the thermal expansion mismatch in the coating systems, and oxidation of bond coats [7-10]. Since thermal barrier coating adherence to the metal substrate is critical, oxide scale growth at the ceramic/bond coat interface and/or at the bond coat/substrate interface will have detrimental effects on the TBC thermal fatigue life. In the

---

† National Research Council — NASA Research Associate at Lewis Research Center.

present study, the oxidation behavior of an air plasma-sprayed FeCrAlY bond coat and 4140 steel substrate is investigated. This FeCrAlY coating system was selected because of the potential compatibility with steel substrates such as in diesel engines. The damage at the interfaces due to oxidation is evaluated based on thermal expansion behavior of the TBC system and the ceramic/metal interface microstructure characterization.

EXPERIMENTAL MATERIALS AND METHODS

The oxidation kinetics of a plasma-sprayed Fe-25Cr-5Al-0.5Y free-standing bond coat ($25 \times 12 \times 3$ mm in size) were characterized by thermogravimetric analysis (TGA) using a Cahn 1000 thermobalance (Mattson Instruments, Madison, WI) in flowing air at 500, 600, 800 and 900°C. These temperatures were chosen as accelerated test conditions compared with actual diesel piston temperatures (typically 300-500°C [4]). The oxidation kinetics of 4140 steel substrate (diameter 12.5×6.5 mm disc specimens) were determined at 400, 500 and 600°C by TGA for the bare specimens, and by measurements of the oxide scale thicknesses from the cross-sections of the FeCrAlY bond coat-wrapped (fully coated on all sides) specimens, respectively.

The thermal expansion experiments were conducted on the TBC systems using an UNITHERM™ Dilatometer system (ANTER CORPORATION, Pittsburgh, PA) in ultra high purity argon and air respectively, as shown in Figure 1. The thickness of the air plasma sprayed ZrO_2-8%Y_2O_3 ceramic coating was 1.5 mm, and that of the FeCrAlY bond coat was chosen as 0.1, 0.5, 0.76 and 1.0 mm respectively. The 4140 steel substrate was 12 mm in thickness to ensure no bending during the experiments. The free-standing ceramic, FeCrAlY bond coat and 4140 steel substrate were also tested under the same conditions.

EXPERIMENTAL RESULTS

Oxidation Kinetics of the TBC System

Figure 2 shows the oxidation weight gains of the air plasma-sprayed FeCrAlY coating. This bond coat exhibited a complicated transient oxidation behavior, probably due to its relatively high porosity and thus increased actual surface area, and the transient oxide growth at these low temperatures. X-ray diffraction results suggest that besides Al_2O_3 scales, there are also some $FeCr_2O_4$ and Cr_2O_3 oxides formed during the initial oxidation stage. The oxidation follows a parabolic rate law after about 30-60 hour initial stage, as can be described by

$$(\Delta w)^2 = w_0^2 + k_p t \tag{1}$$

where Δw is the specific weight gain, k_p is the parabolic rate constant, and w_0 is a constant to account for the fact that the parabolic behavior only occurs after the initial transient

period. Typical SEM micrographs of oxide surface morphology and the cross-section of an oxidized TBC specimen are shown in Figure 3. The oxide whiskers observed on sample surface are believed to be θ-Al_2O_3, which is more stable at these oxidation temperatures. In actual TBC systems, the alumina scale is found to form on the surface as well as the sample laminar splat boundaries. Arrhenius plots of the parabolic rate constants of the FeCrAlY bond coat and the 4140 steel substrate are illustrated in Figure 4 (a) and (b). It can be also noted that, even for FeCrAlY coated 4140 steel specimens, as shown in Figure 4 (b), substantial oxidation occurred at these temperatures.

The oxidation of the bond coat caused interfacial damage. As shown in Figure 5, the oxide growth at the ceramic/bond coat interface initiated the cracking and separation at the ceramic/bond coat interface. Ceramic debonding has been demonstrated for a specimen heavily oxidized at 700°C for 600 hours. The failure mechanism is identified as ceramic micro-cracking near the ceramic/bond coat interface due to oxidation, leading to subsequent extensive ceramic crack propagation in the ceramic coating near the interface. The oxidation at the bond coat/substrate interface also generated interfacial cracks at this interface, as shown in Figure 6. This demonstrates that the porous air plasma sprayed FeCrAlY coating is not very effective in protecting the substrate from oxidation.

Thermal Expansion Behavior of the TBC System

Figure 7 shows the measured thermal expansion behavior of the TBC system. As expected, the 4140 steel substrate and the free-standing ZrO_2-8%Y_2O_3 ceramic coating possess the highest and the lowest thermal expansion coefficients, respectively, while plasma-sprayed FeCrAlY bond coat shows an intermediate thermal expansion coefficient. The thermal expansion behavior of the ceramic coating attached to the substrate is quite different from that of the free-standing ceramic coating. In general, the thermal expansion coefficient of the attached ceramic coating is significantly greater compared to that of a free-standing ceramic coating, but is smaller than that of the substrate.

It is interesting to note that the *in-situ* thermal expansion coefficient of the attached ceramic coating during oxidation cycles decreases with number of cycles in air. Since extremely slow heating and cooling cycles (9.5 hours/cycle at heating and cooling rates about 2-4°C/minute) in air have been used in this thermal expansion experiment, oxidation and thermal expansion mismatch in the system are predominant, and the thermal transient is unimportant. A similar experiment was conducted in ultra high purity argon, and the result showed that the attached ceramic coating had almost a constant thermal expansion coefficient with cycling. The thermal expansion coefficient during the first oxidation cycle in air possesses the highest value, which is essentially the same value measured in argon, suggesting the interface damage effect might not be significant for the first cycle. The FeCrAlY bond coat thermal expansion coefficient showed little difference between argon and air atmospheres, suggesting that the decreasing thermal expansion coefficient of the attached ceramic coating was mainly due to oxidation-induced interface damage rather than to changing bond coat properties.

Figure 8 illustrates the effect of bond coat thickness on the thermal expansion coefficient of the attached ceramic coating. The measured thermal expansion is smaller for the thicker bond coat system. The result suggests the bond coat has isolated substrate thermal strain to some extent for the ceramic coating.
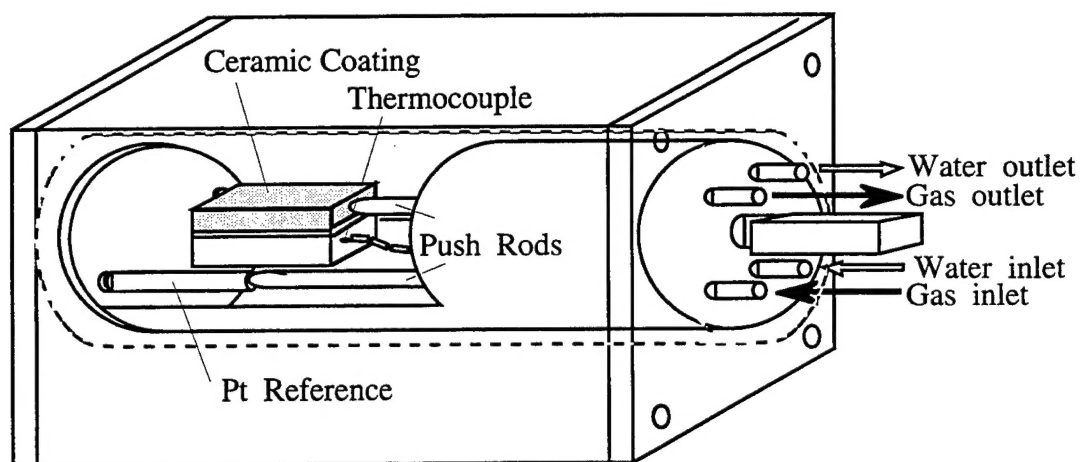
Fig. 1   Schematic diagram showing thermal expansion coefficient measurement of thermal barrier coating systems using dilatometry.
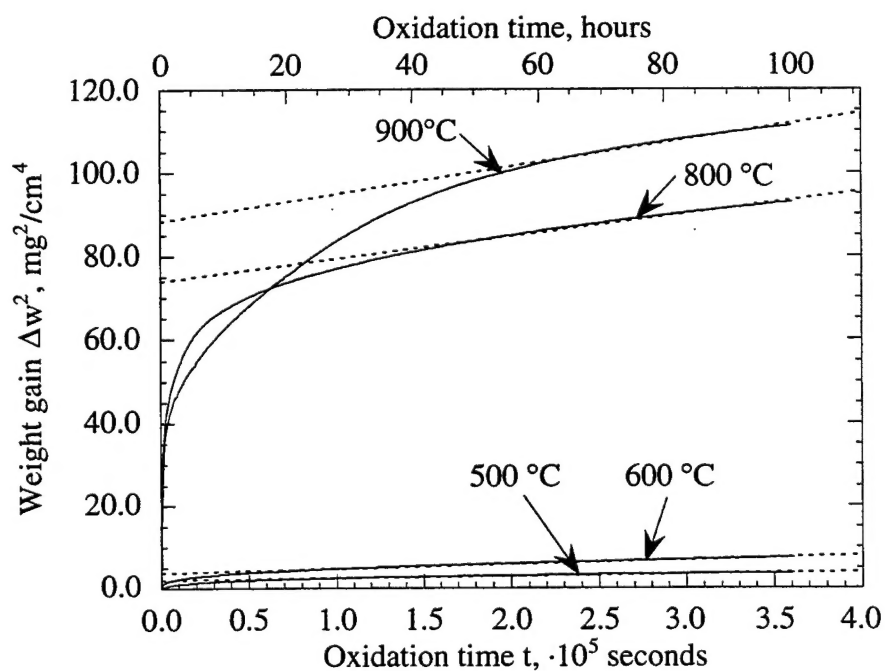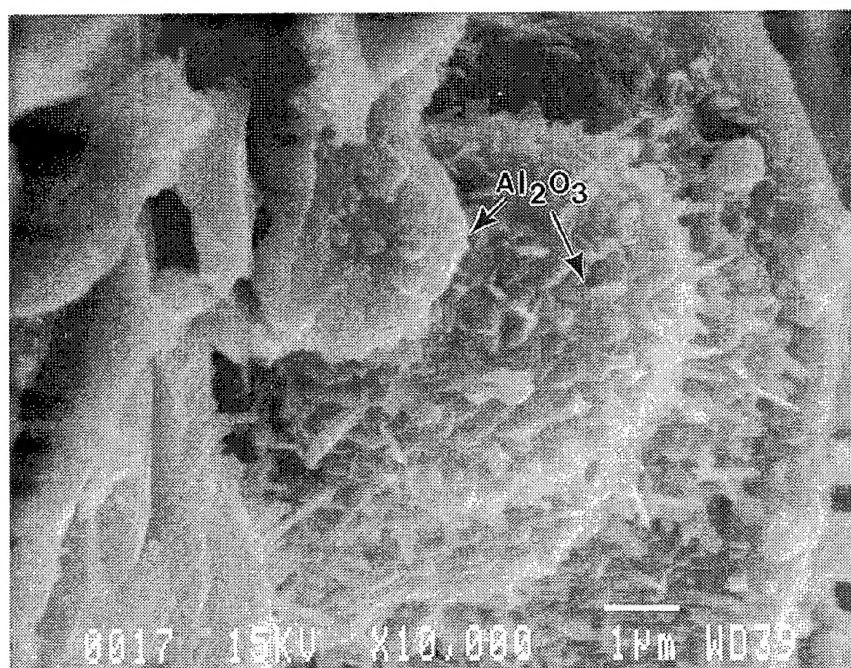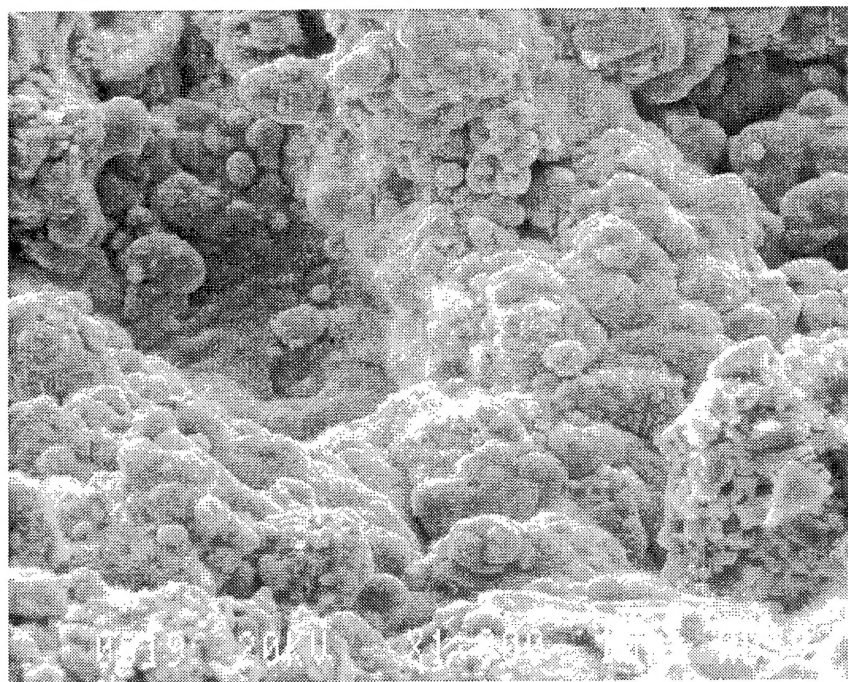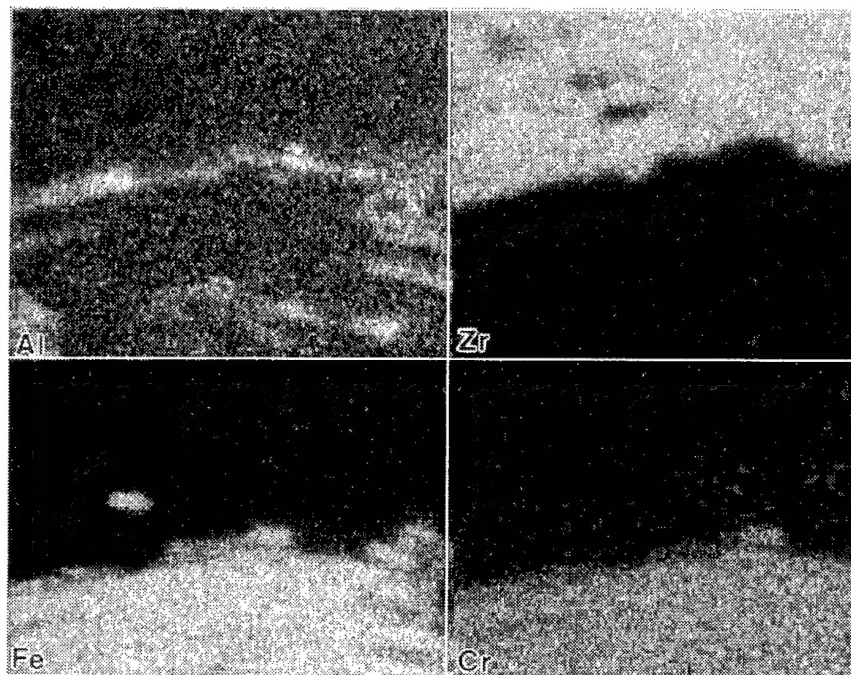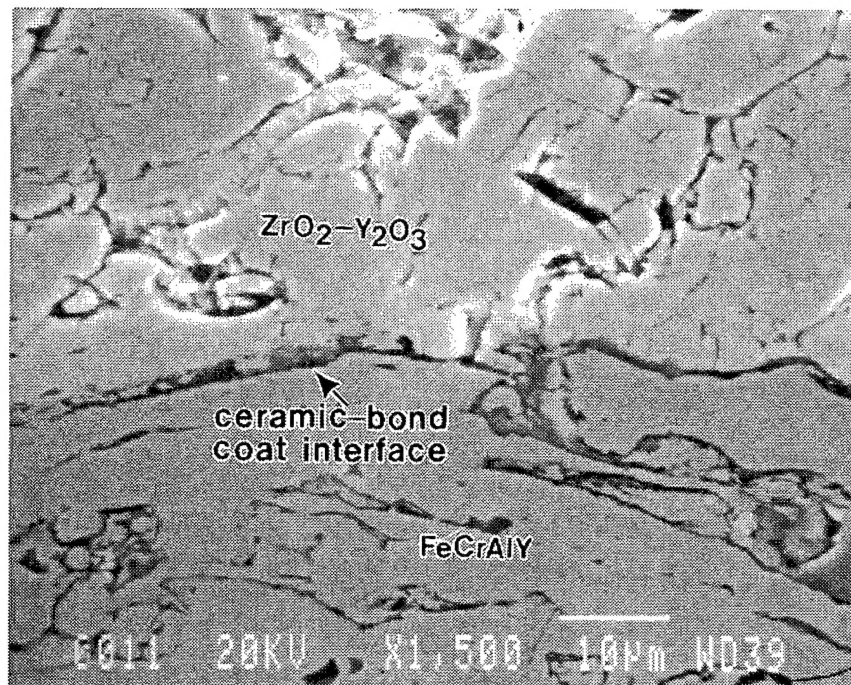

Fig. 2   Oxidation kinetics of atmospheric pressure plasma sprayed Fe-25Cr-5Al-0.5Y coating.

(a) Secondary electron images showing oxide surface morphology.
Fig. 3   SEM micrographs of FeCrAlY bond coat oxidized at 800 °C for 150 hours.

(b) Backscattered electron image and Al, Zr, Fe, Cr X-ray composition maps showing Al_2O_3 grown at the ceramic/bond coat interface and inside bond coat splats.

Fig. 3   SEM micrographs of FeCrAlY bond coat oxidized at 800 °C for 150 hours (continued).
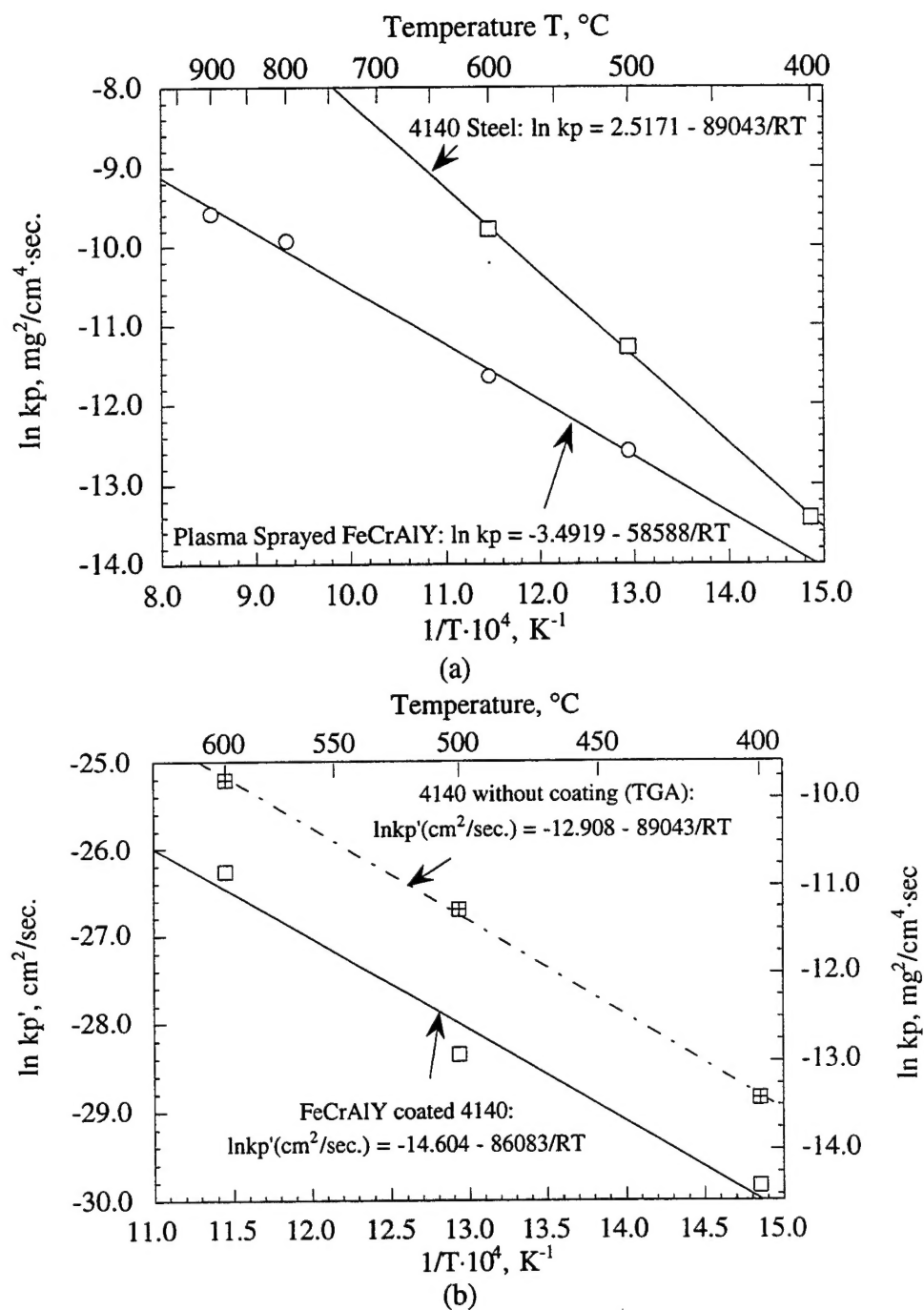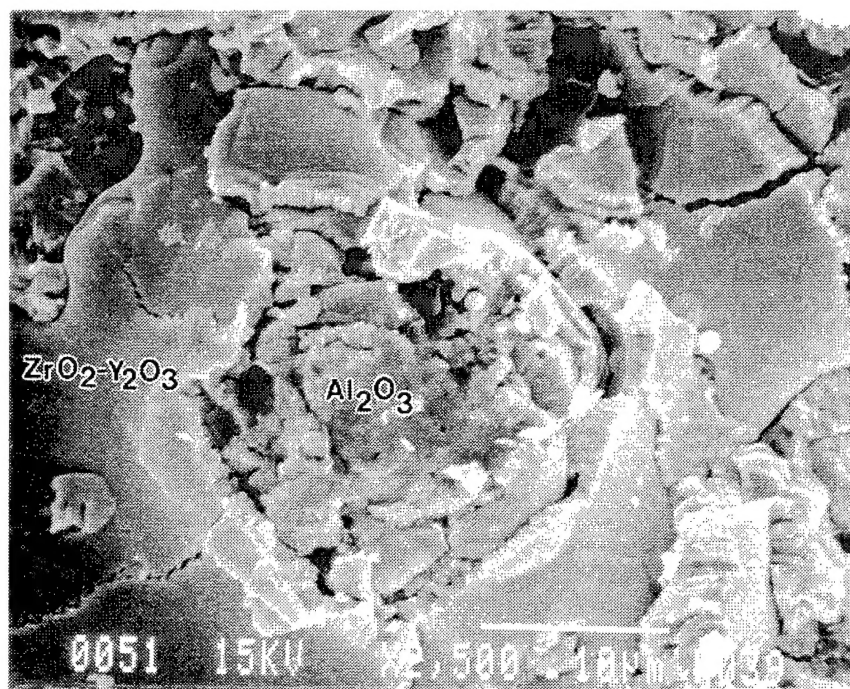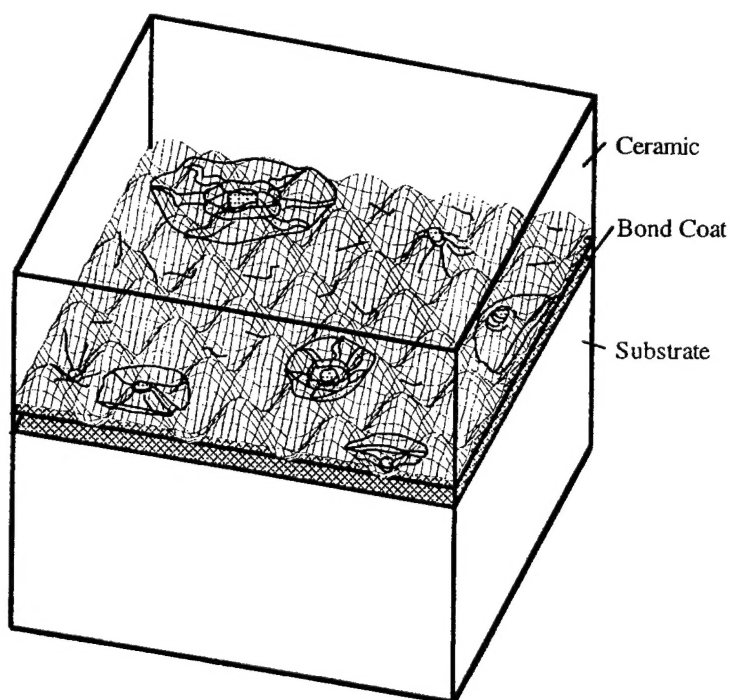
Fig. 4   Arrhenius plots of the parabolic rate constants of the FeCrAlY bond coat and the 4140 steel substrate. (a) ln k_p (in mg²/cm⁴·sec) - 1/T relations for the free standing FeCrAlY and 4140 steel specimens by TGA measurements; (b) ln k_p' (in cm²/sec) - 1/T relation for 4140 steel specimens with and without FeCrAlY bond coat by scale thickness measurements.

7

(a)

(b)

Fig. 5 Ceramic coating failure due to the FeCrAlY bond coat oxidation. (a) SEM micrograph showing ceramic coating cracking and spallation at the ceramic/bond coat interface; (b) Schematic diagram of the ceramic coating failure mechanism.
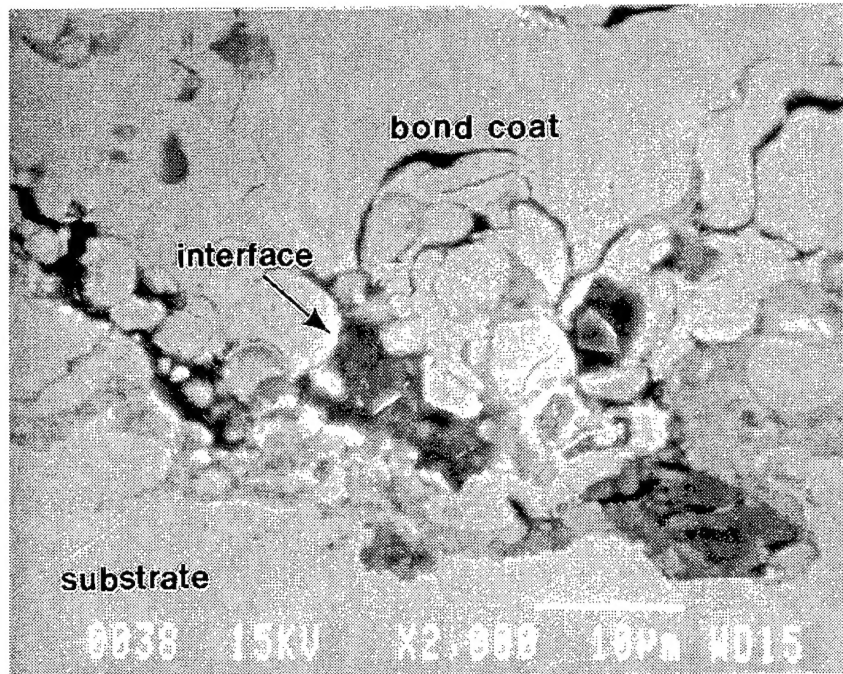
Fig. 6 The bond coat/substrate interface cracking due to the substrate oxidation at 500 °C for 336 hours.
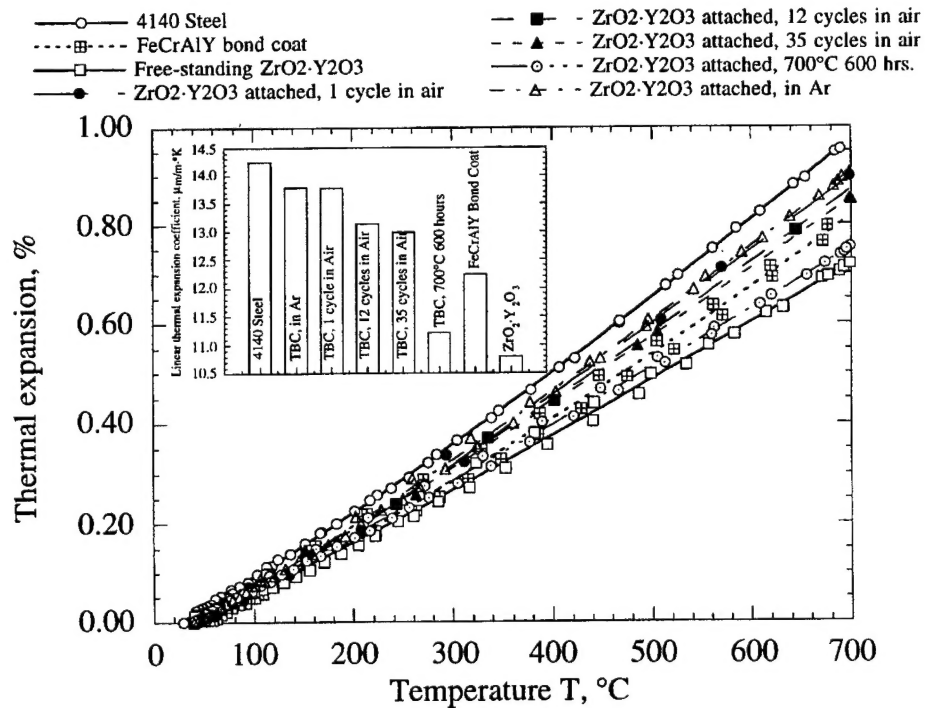

Fig. 7 Thermal expansion behavior of the thermal barrier coating system.
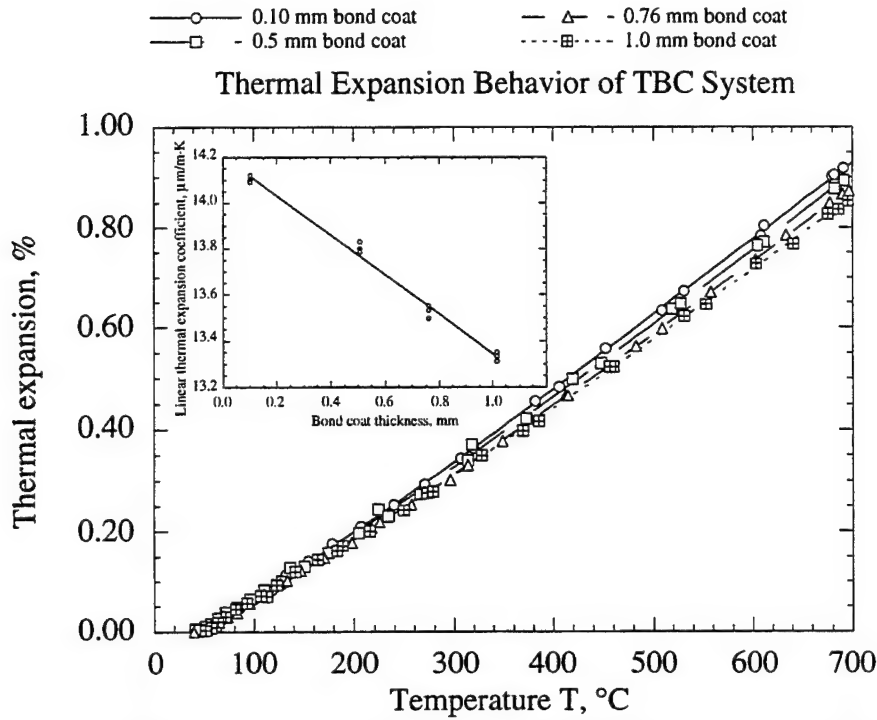
9

Fig. 8   The effect of bond coat thickness on thermal expansion coefficient of the TBC system.

DISCUSSION

In a thermal barrier coating system, the bond coat will act as a graded thermal expansion layer to reduce the thermal expansion mismatch between the ceramic layer and the substrate. It will also provide good bonding strength between them. The bond coat may also be able to relieve cyclic stresses through plastic deformation. Early dilatometry experiments showed that the thermal expansion coefficients of ceramic coatings on steel substrates were significantly influenced by the substrates and bond coats [11]. In general, the thermal expansion characteristics of ceramic coatings attached to substrates behaved more or less the same as those of the bond coats. Therefore, in order to quantify the strain isolation effect and bond adhesion strength of the bond coat, two parameters: strain isolation coefficient, S_i, and normalized adhesion coefficient, A_i, are introduced in this study. These are described in Appendix 1. S_i reveals the intrinsic bond coat effectiveness in isolating thermal strain for the ceramic coatings, and A_i reflects the integrity of the interface, which is *normalized* to the amount of damage present during the first heating cycle where the extent of interfacial cracking damage is usually small. The two parameters can be expressed as

$$S_i = \frac{\alpha_s - \alpha_c^{att,i}}{\alpha_s - \alpha_c^0} \tag{2}$$

10

$$A_i = \frac{\alpha_c^{att,i} - \alpha_c^0}{\alpha_c^{att,1} - \alpha_c^0} \tag{3}$$

where α_s and α_c^0 are linear thermal expansion coefficients of the substrate and the free-standing ceramic coating, $\alpha_c^{att,1}$ and $\alpha_c^{att,i}$ are the thermal expansion coefficients of the ceramic layer attached on the substrate surface in the first cycle and the ith cycle respectively. These expressions arise from the assumption that, with the case of no debonding and no strain isolation provided by the bond coat, the ceramic will stretch and contract via crack opening/closing and/or splat sliding (This displacement is assumed to occur uniformly across the ceramic layer thickness). Thus, for no strain isolation $S_i = 0$, and no debonding $A_i = 1$. On the other hand, $S_i = 1$ means complete strain isolation, and $A_i = 0$ indicates a complete debonding at the interface. It can be expected that S_i depends on bond coat thermal properties and thickness, while A_i is mainly dependent upon interfacial properties. Since no debonding is most likely in the first heating cycle (as has been confirmed in the experiments), S_1 is effectively a measure of initial strain isolation provided by the bond coat. Bond coat and substrate oxidation will have significant effect on the adhesion properties.

Figure 9 shows the initial strain isolation coefficient S_i of the TBC system as a function of the bond coat thickness. From the thermal expansion experiments, it can be seen that the strain isolation effect increases substantially with the bond coat thickness. From the simple elastic model derived in Appendix 2, the thermal expansion coefficient of the attached ceramic coating can be written as

$$\alpha_c^{att} = \alpha_c^0 + \frac{(\alpha_b - \alpha_c)E_b(1 - v_c)(1 - v_s)t_b + (\alpha_s - \alpha_c)E_s(1 - v_c)(1 - v_b)t_s}{E_c t_c(1 - v_b)(1 - v_s) + E_b t_b(1 - v_c)(1 - v_s) + E_s t_s(1 - v_c)(1 - v_b)} \tag{4}$$

where α_b is linear thermal expansion coefficient of the bond coat, E's and v's are the Young's Moduli and the Poisson's ratios for the ceramic coating, the bond coat and the substrate respectively, and t_c, t_b and t_s are thicknesses of the ceramic coating, the bond coat and the substrate. Equation (4) suggests the strain isolation by a thin bond coat will not be significant with a predominantly thick substrate. The strain isolation coefficient as a function of bond coat thickness, which is calculated from Equations (2) and (4), is also illustrated in Figure 9. The discrepancy between the experimental data and theoretical calculation may be due to the strain distributions in the system, which is probably associated with the specimen edge effect and the unique compliant bond coat behavior. Uncertainties in the elastic properties such as elastic moduli in the system may also affect the strain isolation coefficient. However, as shown in Figure 9, even if the value of E_c is changed from 10 to 60 GPa, the theoretical value of S_i would increase only by about 0.03.

The interface damage due to oxidation has been evaluated by *in-situ* measurement of the thermal expansion of ceramic coating on steel substrate in flowing air, as illustrated in

11

Fig. 10. It can be seen that the adhesion coefficient A_i decreases with increasing oxidation time. The adhesion coefficient is closely related to the maximum interfacial shear stress behavior (Appendix 3). Therefore it is a good measure of residual interfacial strength. It can be seen that the adhesion coefficient A_i has decreased from an initial value of 1 in the first cycle to about 0.75 after 35 cycles. For the specimen oxidized at 700°C for 600 hours, A_i has dropped to about 0.15. The results confirm that oxidation has a strong detrimental effect on TBC interfacial adherence.

CONCLUDING REMARKS

The oxidation of the bond coat and the substrate has been shown to have detrimental effect on the ceramic coating adherence to the substrate. A method based on dilatometry has been established to quantitatively evaluate the interfacial damage due to the oxidation of the thermal barrier coating system. This approach will help to develop strategies for advanced TBC design, and to evaluate the effect of bond coat mechanical and oxidation properties on TBC fatigue life.

For the TBC system and experimental conditions studied, the interface adhesion coefficient has reduced from an initial value of 1 during the first cycle to about 0.75 after 35 oxidation cycles. It was also found that the strain isolation effect could be improved by increasing the FeCrAlY bond coat thickness. The strain isolation coefficient increased from about 0.04 to 0.25, as the bond coat thickness changed from 0.1 to 1.0 mm. It may be possible to design optimum values of strain isolation S_i and interface adhesion A_i in order to achieve the best TBC performance.
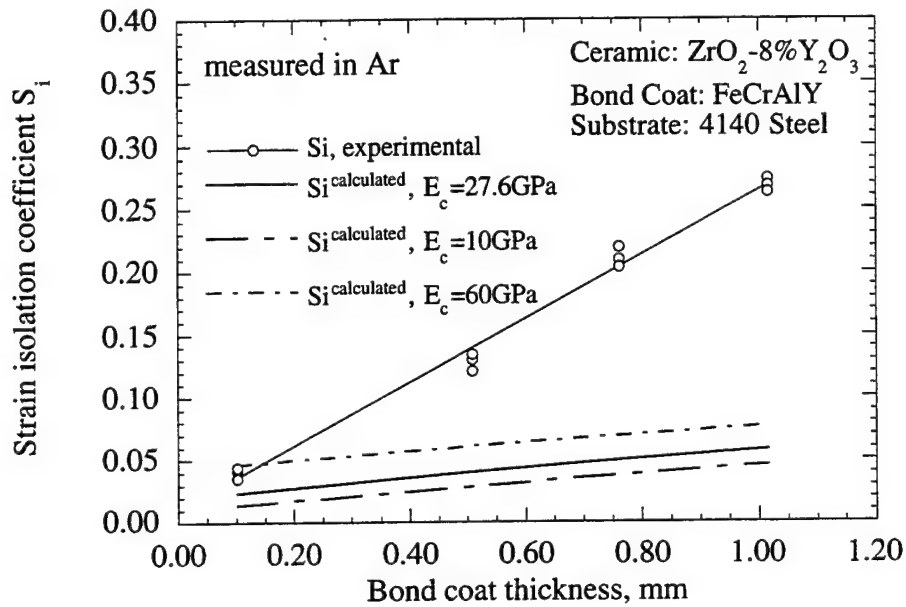
ACKNOWLEDGMENT

Fig. 9 Strain isolation effect as a function of the bond coat thickness. The elastic properties used for the calculation of A_i (solid line) are: $E_c = 27.6$ GPa, $E_b = 137.9$ GPa, $E_s = 175.8$ GPa, $v_c = 0.25$, $v_b = 0.27$ and $v_s = 0.25$, as reported in reference [12].

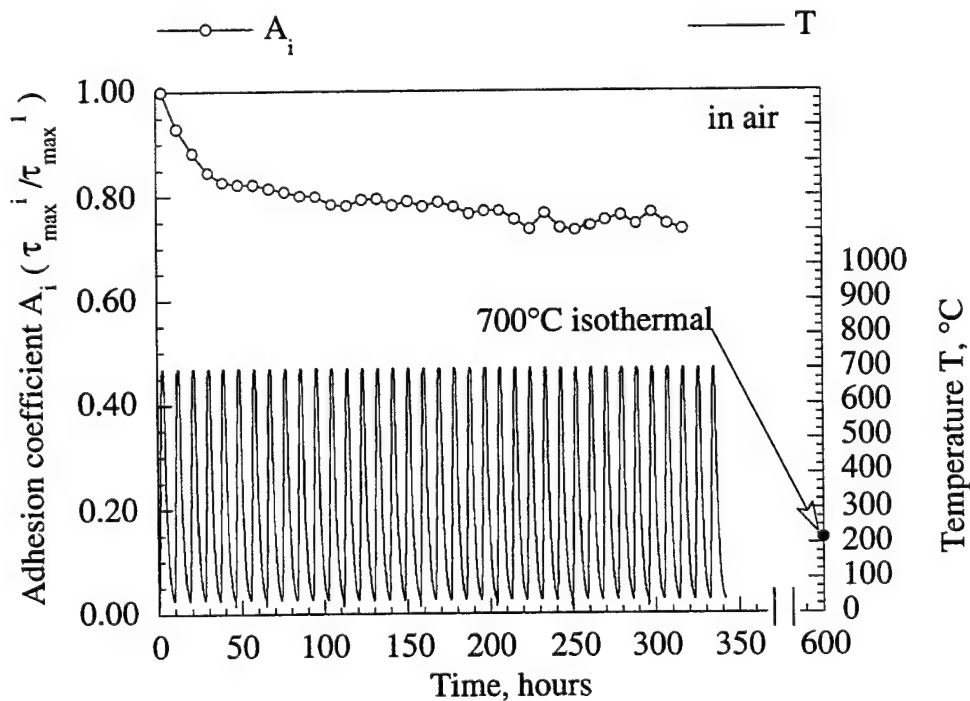

Fig. 10 Adhesion coefficient as a function of oxidation time.

13

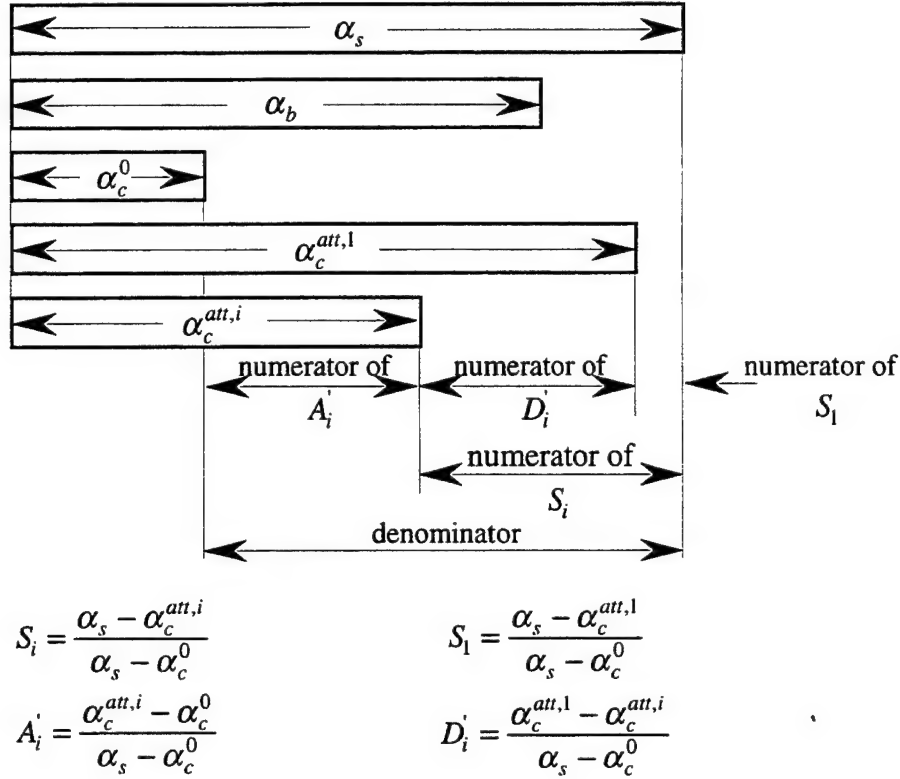## Appendix 1. Strain Isolation Coefficient and Interface Adhesion Coefficient

$$S_i = \frac{\alpha_s - \alpha_c^{att,i}}{\alpha_s - \alpha_c^0} \qquad\qquad S_1 = \frac{\alpha_s - \alpha_c^{att,1}}{\alpha_s - \alpha_c^0}$$

$$A_i^{'} = \frac{\alpha_c^{att,i} - \alpha_c^0}{\alpha_s - \alpha_c^0} \qquad\qquad D_i^{'} = \frac{\alpha_c^{att,1} - \alpha_c^{att,i}}{\alpha_s - \alpha_c^0}$$

Fig. A1   Definition of strain isolation coefficient S_i, adhesion coefficient $A_i^{'}$ and damage coefficient $D_i^{'}$.

The strain isolation and interface adhesion in a TBC system can be evaluated from the thermal expansion behavior of the system. As illustrated in Figure A1, the linear expansion coefficients of the free-standing ceramic and substrate are α_c^0 and α_s respectively. It is assumed that during the ith cycle, the expansion of the attached ceramic $\alpha_c^{att,i}$ would stretch to equal the expansion of dominant substrate if the bond coat provides no strain isolation. It is further assumed that the expansion coefficient of the attached ceramic would be as low as that of the free-standing ceramic if the bond coat provided complete strain isolation (This assumes that interfacial cracking is not contributing to the measured strain isolation). Therefore, the experimentally determined attached ceramic thermal expansion coefficient is bounded by

$$\alpha_c^0 \leq \alpha_c^{att,i} \leq \alpha_s \qquad\qquad (A1)$$

and, the ratio of the measured differential thermal expansion during the ith cycle to the

theoretical maximum $\alpha_s - \alpha_c^0$ is

$$S_i = \frac{\alpha_s - \alpha_c^{att,i}}{\alpha_s - \alpha_c^0}$$ (A2)

where S_i is, by definition the strain isolation factor. For cycle 1 (where the assumption of minimal cracking is strongest):

$$S_1 = \frac{\alpha_s - \alpha_c^{att,1}}{\alpha_s - \alpha_c^0}$$ (A3)

The measured value of $\alpha_c^{att,i}$ may decrease with cycling if interfacial cracking is occurring with the lower limit being the value α_c^0 for the free-standing ceramic. Therefore, the experimentally determined ceramic thermal expansion coefficient is bounded by

$$\alpha_c^0 \leq \alpha_c^{att,i} \leq \alpha_s^{att,1}$$ (A4)

Thus, the ratio of the *remaining* stretch amount for the attached ceramic during the ith cycle to the theoretical maximum $\alpha_s - \alpha_c^0$ is defined as adhesion coefficient $A_i^{'}$, which can be written as

$$A_i^{'} = \frac{\alpha_c^{att,i} - \alpha_c^0}{\alpha_s - \alpha_c^0}$$ (A5)

Similarly, the ratio of the *lost* stretch amount for the coating under the ith cycle to the maximum differential expansion $\alpha_s - \alpha_c^0$ is defined as interfacial damage coefficient $D_i^{'}$

$$D_i^{'} = \frac{\alpha_c^{att,1} - \alpha_c^{att,i}}{\alpha_s - \alpha_c^0}$$ (A6)

Note that $S_1 + A_i^{'} + D_i^{'} = 1$ and $S_i = S_1 + D_i^{'}$. These expressions suggest that the parameters S_1, $A_i^{'}$ and $D_i^{'}$ have accounted for the total difference between the thermal expansion coefficients of the substrate and the free-standing ceramic coating; In addition, the strain isolation coefficient in the ith cycle S_i could include the contributions from the intrinsic

strain isolation S_1 and interface cracking damage D_i during the oxidation cycles. Thus, the amount of ceramic stretch in the ith cycle normalized to the amount of stretch during the first cycle may be defined as *normalized* adhesion coefficient A_i

$$A_i = \frac{A_i'}{A_i' + D_i'} = \frac{\alpha_c^{att,i} - \alpha_c^0}{\alpha_c^{att,1} - \alpha_c^0} \tag{A7}$$

Appendix 2.   Thermal Expansion Behavior in Thermal Barrier Coating Systems

When temperature is changed from T_0 to T_1, the thermal strains ε_c^{th}, ε_b^{th} and ε_s^{th} for ceramic coating, bond coat and substrate are given by

$$\varepsilon_c^{th} = \alpha_c(T_1 - T_0) \tag{A8a}$$

$$\varepsilon_b^{th} = \alpha_b(T_1 - T_0) \tag{A8b}$$

$$\varepsilon_s^{th} = \alpha_s(T_1 - T_0) \tag{A8c}$$

where α_c, α_b and α_s are the thermal expansion coefficients of ceramic, bond coat and substrate respectively. Providing no bending is present in the system, the elastic strains ε_c^e, ε_b^e and ε_s^e in the constrained thermal barrier coating system can be expressed as

$$\varepsilon_c^e = \sigma_c\left(\frac{1 - v_c}{E_c}\right) \tag{A9a}$$

$$\varepsilon_b^e = \sigma_b\left(\frac{1 - v_b}{E_b}\right) \tag{A9b}$$

$$\varepsilon_s^e = \sigma_s\left(\frac{1 - v_s}{E_s}\right) \tag{A9c}$$

where σ_c, σ_b and σ_s are stresses in the ceramic, bond coat and the substrate respectively, E and v with subscripts c, b and s are the Young's Moduli and the Poisson's ratios of the ceramic, bond coat and the substrate. Strain compatibility and force balance result in the following relations

16

$$\sigma_c\left(\frac{1-v_c}{E_c}\right)+\alpha_c\Delta T = \sigma_b\left(\frac{1-v_b}{E_b}\right)+\alpha_b\Delta T = \sigma_s\left(\frac{1-v_c}{E_c}\right)+\alpha_s\Delta T \tag{A10}$$

$$\int_0^{t_c}\sigma_c\cdot dt+\int_0^{t_b}\sigma_b\cdot dt+\int_0^{t_s}\sigma_s\cdot dt = 0 \tag{A11}$$

Where t_c, t_b and t_s are thicknesses of the ceramic coating, the bond coat and the substrate, respectively. From Equations (A10) and (A11), the elastic stresses and elastic strains in the thermal barrier coating system can be obtained

$$\sigma_c = \frac{(\alpha_b-\alpha_c)\Delta TE_bE_c(1-v_s)t_b+(\alpha_s-\alpha_c)\Delta TE_sE_c(1-v_b)t_s}{E_ct_c(1-v_b)(1-v_s)+E_bt_b(1-v_c)(1-v_s)+E_st_s(1-v_c)(1-v_b)} \tag{A12}$$

$$\sigma_b = \frac{\left[(\alpha_b-\alpha_c)\Delta TE_b(1-v_s)t_b+(\alpha_s-\alpha_c)\Delta TE_s(1-v_b)t_s\right]E_b(1-v_c)}{(1-v_b)\left[E_ct_c(1-v_b)(1-v_s)+E_bt_b(1-v_c)(1-v_s)+E_st_s(1-v_c)(1-v_b)\right]}$$

$$-\frac{(\alpha_b-\alpha_c)\Delta TE_b}{1-v_b} \tag{A13}$$

$$\sigma_s = \frac{\left[(\alpha_b-\alpha_c)\Delta TE_b(1-v_s)t_b+(\alpha_s-\alpha_c)\Delta TE_s(1-v_b)t_s\right]E_s(1-v_c)}{(1-v_s)\left[E_ct_c(1-v_b)(1-v_s)+E_bt_b(1-v_c)(1-v_s)+E_st_s(1-v_c)(1-v_b)\right]}$$

$$-\frac{(\alpha_s-\alpha_c)\Delta TE_s}{1-v_s} \tag{A14}$$

$$\varepsilon_c^e = \frac{(\alpha_b-\alpha_c)\Delta TE_b(1-v_c)(1-v_s)t_b+(\alpha_s-\alpha_c)\Delta TE_s(1-v_c)(1-v_b)t_s}{E_ct_c(1-v_b)(1-v_s)+E_bt_b(1-v_c)(1-v_s)+E_st_s(1-v_c)(1-v_b)} \tag{A15}$$

$$\varepsilon_b^e = \frac{\left[(\alpha_b-\alpha_c)\Delta TE_b(1-v_s)t_b+(\alpha_s-\alpha_c)\Delta TE_s(1-v_b)t_s\right](1-v_c)}{E_ct_c(1-v_b)(1-v_s)+E_bt_b(1-v_c)(1-v_s)+E_st_s(1-v_c)(1-v_b)}$$

$$-(\alpha_b-\alpha_c)\Delta T \tag{A16}$$

$$\varepsilon_s^e = \frac{\left[(\alpha_b-\alpha_c)\Delta TE_b(1-v_s)t_b+(\alpha_s-\alpha_c)\Delta TE_s(1-v_b)t_s\right](1-v_c)}{E_ct_c(1-v_b)(1-v_s)+E_bt_b(1-v_c)(1-v_s)+E_st_s(1-v_c)(1-v_b)}$$

$$-\left(\alpha_s - \alpha_c\right)\Delta T \tag{A17}$$

where $\Delta T = T_1 - T_0$. Therefore, the thermal expansion coefficient of the ceramic coating attached to the substrate can be written as

$$\alpha_c^{att} = \frac{\alpha_c^0 \Delta T + \varepsilon_c^e}{\Delta T}$$

$$= \alpha_c^0 + \frac{\left(\alpha_b - \alpha_c\right)E_b(1-v_c)(1-v_s)t_b + \left(\alpha_s - \alpha_c\right)E_s(1-v_c)(1-v_b)t_s}{E_c t_c(1-v_b)(1-v_s) + E_b t_b(1-v_c)(1-v_s) + E_s t_s(1-v_c)(1-v_b)} \tag{A18}$$

Appendix 3. The relation between adhesion coefficient A_i and interfacial shear stress ratio $\tau_{max}^i / \tau_{max}^1$

The thermal elastic strain exerted on the ceramic coating in the TBC system during temperature change is dependent on the effective load transfer at the ceramic/bond coat interface. In the case of linear shear stress distribution at the interface, as originally suggested by Tien and Davidson [13], the force balance and thus the maximum shear stress can be expressed by

$$\int_0^{L/2} \tau dx = \frac{\tau_{max}}{4}L = t_c\left(\frac{\varepsilon_c^e E_c}{1-v_c}\right) \tag{A19a}$$

$$\tau_{max} = \frac{4t_c}{L}\left(\frac{\varepsilon_c^e E_c}{(1-v_c)}\right) = \frac{4t_c}{L}\left(\frac{\left(\alpha_c^{att} - \alpha_c^0\right)\Delta T E_c}{\left(1 + \dfrac{E_c\, t_c}{E_s\, t_s}\right)(1-v_c)}\right) \tag{A19b}$$

where L is the specimen length. Therefore, the maximum shear stress ratio $\tau_{max}^i / \tau_{max}^1$ under the first cycle and the ith cycle is given by

$$\frac{\tau_{max}^i}{\tau_{max}^1} = \frac{\alpha_c^{att,i} - \alpha_c^0}{\alpha_c^{att,1} - \alpha_c^0} = A_i \tag{A20}$$

Equation (A20) indicates that the interfacial adhesion coefficient in the system is equivalent to the maximum interfacial shear stress ratio.

18

REFERENCES

[1] D. L. Ruckel, Thin Solid Films, **73**, 455 (1980).

[2] R. A. Miller, Surface and Coatings Technology, **30**, 1 (1987).

[3] R. A. Miller, in Thermal Barrier Coating Workshop, W. J. Brindley, Editor, p.17, Cleveland, Ohio (1995).

[4] M. B. Beardsley and H. J. Larson, DOE/NASA/0332-1, NASA CR-190759, August (1992).

[5] P. M. Pierz, Surface and Coating Technology, **61**, 60 (1993).

[6] R. A. Miller, NASA TM-103130, DOE/NASA/21794-1, May (1990).

[7] C. C. Berndt and R. A. Miller, in Proceedings of the 8th Annual Conference on Composites and Advanced Ceramic Materials, W. J. Smothers, Editor, p.479, The American Ceramic Society, Inc., Columbus, Ohio (1984).

[8] R. A. Miller, Journal of the American Ceramic Society, **67**, 517 (1984).

[9] S. Stecura, NASA TM-87062, July (1985).

[10] W. J. Brindley, in Thermal Barrier Coating Workshop, W. J. Brindley, Editor, p.189, Cleveland, Ohio (1995).

[11] S. Rangaswamy, H. Herman and S. Safai, Thin Solid Films, **73**, 43 (1980).

[12] G. C. Chang, W. Phucharoen and R. A. Miller, Surface and Coatings Technology, **32**, 307 (1987).

[13] J. K. Tien and J. M. Davidson, in Stress Effects and the Oxidation of Metals, J. V. Cathcart, Editor, p.200, The Metallurgical Society of AIME, Oak Ridge, Tennessee (1974).

REPORT DOCUMENTATION PAGE

Public reporting burden for this collection of information is estimated to average 1 hour per response, including the time for reviewing instructions, searching existing data sources, gathering and maintaining the data needed, and completing and reviewing the collection of information. Send comments regarding this burden estimate or any other aspect of this collection of information, including suggestions for reducing this burden, to Washington Headquarters Services, Directorate for Information Operations and Reports, 1215 Jefferson Davis Highway, Suite 1204, Arlington, VA 22202-4302, and to the Office of Management and Budget, Paperwork Reduction Project (0704-0188), Washington, DC 20503.

1. AGENCY USE ONLY (Leave blank)	2. REPORT DATE	3. REPORT TYPE AND DATES COVERED
	November 1996	Technical Memorandum

4. TITLE AND SUBTITLE

Evaluation of Oxidation Damage in Thermal Barrier Coating Systems

5. FUNDING NUMBERS

WU–505–63–52
1L161102AH45

6. AUTHOR(S)

Dongming Zhu and Robert A. Miller

7. PERFORMING ORGANIZATION NAME(S) AND ADDRESS(ES)

NASA Lewis Research Center
Cleveland, Ohio 44135–3191
and
Vehicle Propulsion Directorate
U.S. Army Research Laboratory
Cleveland, Ohio 44135–3191

8. PERFORMING ORGANIZATION REPORT NUMBER

E–10518

9. SPONSORING/MONITORING AGENCY NAME(S) AND ADDRESS(ES)

National Aeronautics and Space Administration
Washington, DC 20546–0001
and
U.S. Army Research Laboratory
Adelphi, Maryland 20783–1145

10. SPONSORING/MONITORING AGENCY REPORT NUMBER

NASA TM–107360
ARL–TR–1254

11. SUPPLEMENTARY NOTES

12a. DISTRIBUTION/AVAILABILITY STATEMENT

Unclassified - Unlimited
Subject Category 26

This publication is available from the NASA Center for AeroSpace Information, (301) 621–0390.

12b. DISTRIBUTION CODE

13. ABSTRACT (Maximum 200 words)

A method based on the technique of dilatometry has been established to quantitatively evaluate the interfacial damage due to the oxidation in a thermal barrier coating system. Strain isolation and adhesion coefficients have been proposed to characterize the thermal barrier coating (TBC) performance based on its thermal expansion behavior. It has been found that, for a thermal barrier coating system consisting of ZrO_2-8%Y_2O_3/FeCrAlY/4140 steel substrate, the oxidation of the bond coat and substrate significantly reduced the ceramic coating adherence, as inferred from the dilatometry measurements. The *in-situ* thermal expansion measurements under 30 °C to 700 °C thermal cycling in air showed that the adhesion coefficient, A_i, decreased by 25% during the first 35 oxidation cycles. Metallography showed that delamination occurred at both the ceramic/bond coat and bond coat/substrate interfaces. In addition, the strain isolation effect has been improved by increasing the FeCrAlY bond coat thickness. The strain isolation coefficient, S_i, increased from about 0.04 to 0.25, as the bond coat thickness changed from 0.1 mm to 1.0 mm. It may be possible to design optimum values of strain isolation and interface adhesion coefficients to achieve the best TBC performance.

14. SUBJECT TERMS

Thermal barrier coating; Dilatometry; Thermal expansion; Interface adhesion; Oxidation damage; Strain isolation

15. NUMBER OF PAGES

21

16. PRICE CODE

A03

17. SECURITY CLASSIFICATION OF REPORT	18. SECURITY CLASSIFICATION OF THIS PAGE	19. SECURITY CLASSIFICATION OF ABSTRACT	20. LIMITATION OF ABSTRACT
Unclassified	Unclassified	Unclassified	